

Mitochondrial degeneration in dystrophic neurites of senile plaques may lead to extracellular deposition of fine filaments

John C. Fiala · Marcia Feinberg · Alan Peters · Helen Barbas

Received: 29 March 2007 / Accepted: 10 July 2007 / Published online: 17 August 2007
© Springer-Verlag 2007

Abstract Recent data show that amyloid precursor protein accumulates inside axons after disruption of fast axonal transport, but how this leads to mature plaques with extracellular amyloid remains unclear. To investigate this issue, primitive plaques in prefrontal cortex of aged rhesus monkeys were reconstructed using serial section electron microscopy. The swollen profiles of dystrophic neurites were found to be diverticula from the main axis of otherwise normal neurites. Microtubules extended from the main neurite axis into the diverticulum to form circular loops or coils, providing a transport pathway for trapping organelles. The quantity and morphology of organelles contained within diverticula suggested a progression of degeneration. Primitive diverticula contained microtubules and normal mitochondria, while larger, presumably older, diverticula contained large numbers of degenerating mitochondria. In advanced stages of degeneration, apparent autophagosomes derived from mitochondria exhibited a loose lamellar to filamentous internal structure. Similar filamentous material and remnants of mitochondria were visible in the

extracellular spaces of plaques. This progression of degeneration suggests that extracellular filaments originate inside degenerating mitochondria of neuritic diverticula, which may be a common process in diverse diseases.

Keywords Aging · Alzheimer's disease · Amyloid- β · Autophagocytosis · Axonal transport · Synapse · Ultrastructure

Introduction

Neuritic plaques, containing clusters of dystrophic neurites and extracellular fibrillar amyloid, are a common form of degeneration in the brain. Neuritic plaques occur in Alzheimer's disease, Creutzfeldt–Jakob disease, traumatic brain injury, and after poisoning with various metals (Tomlinson 1992). Neuritic plaques also occur during normal aging in humans and other primates (Peters 1991; Wisniewski et al. 1973). In aged monkeys, the plaque amyloid is made up of amyloid- β protein while the dystrophic neurites contain accumulations of amyloid- β precursor protein (Kimura et al. 2003; Martin et al. 1991, 1994; Uno et al. 1996). How accumulation of intraneuronal amyloid- β precursor protein relates to extracellular amyloid in the plaque remains unclear.

In their classic ultrastructural studies, Terry and Wisniewski (1970, 1972) suggested that the earliest precursor of a senile plaque is an abnormally swollen neurite filled with numerous mitochondria and lamellar and dense bodies. They proposed that plaques develop from small clusters of these dystrophic neurites. These *primitive plaques* would then mature into *classical plaques* with cores of extracellular amyloid surrounded by dystrophic neurites, and subsequently evolve into *compact (burnt-out)* plaques, consisting

J. C. Fiala (✉) · M. Feinberg · H. Barbas
Department of Health Sciences, Boston University,
635 Commonwealth Ave., Boston, MA 02215, USA
e-mail: fiala@bu.edu

A. Peters · H. Barbas
Program in Neuroscience, Boston University,
Boston, MA 02215, USA

A. Peters · H. Barbas
Department of Anatomy and Neurobiology,
Boston University School of Medicine,
Boston, MA 02118, USA

H. Barbas
New England Primate Research Center,
Harvard Medical School, Boston, MA 02115, USA

mostly of fibrillar amyloid surrounded by glia. Alternative hypotheses propose either that plaques of one type do not evolve into any other type or that the reverse progression occurs with compact plaques evolving into primitive ones (Armstrong 1998; Weigel et al. 2000).

Exactly what initiates plaque formation is unknown, but one proposal is that axonal swellings form because of disruption of axonal transport (Coleman 2005; Götz et al. 2006; Gouras et al. 2005; Kidd 1964; Praprotnik et al. 1996a; Stokin and Goldstein 2006; Terry and Wisniewski 1972). In this scenario, axonal swellings accumulate amyloid- β precursor protein intracellularly and lysis of swellings ultimately leads to the extracellular deposition of amyloid- β peptide. Extracellular accumulation of amyloid- β then produces further disruption in axonal transport and the plaque continues to expand. In this hypothesis it is unclear in which intracellular compartment amyloid- β forms, but recent evidence suggests that mitochondria may be involved in amyloid- β pathology in Alzheimer's disease (Caspersen et al. 2005; Devi et al. 2006; Hirai et al. 2001; Lustbader et al. 2004; Manczak et al. 2006; Rui et al. 2006; Yan et al. 2006).

We examined this issue by investigating the fine structure of neuritic swellings of senile plaques in the prefrontal cortex of aged monkeys using three-dimensional reconstruction of serial sections to delineate the stages of degeneration to a greater degree than has been possible using single-section ultrastructural analysis. We provide novel evidence consistent with disorganization of microtubule transport mechanisms and mitochondrial degeneration leading to disintegration of neuritic swellings and deposition of filamentous material in the extracellular space.

Materials and methods

Data were obtained from pieces of dorsal area 8 in prefrontal cortex, taken from two rhesus monkeys (*Macaca mulatta*) 32 years of age, one male and one female. These animals were approximately equivalent to 90–100 year-old humans, and were chosen because area 8 of prefrontal cortex in these monkeys exhibited numerous plaques. The fine structural characteristics of layers II–III of area 8 in these two animals were similar to those of other old animals we have examined.

Details of the fixation and tissue processing protocols were described previously (Peters et al. 1994). Intra-aortic perfusions, carried out in accordance with the approved Institutional Animal Care and Use Committee regulations, used 1% paraformaldehyde and 1.25% glutaraldehyde in 0.1 M cacodylate buffer at pH 7.4. After initial fixation, the brain was removed and fixed further by immersion in a cold solution of 2% paraformaldehyde and 2.5%

glutaraldehyde in 0.1 M cacodylate buffer at pH 7.4 until tissue samples were taken. Tissue samples containing the entire depth of cortex were osmicated, dehydrated in an ascending series of alcohols, and embedded in Araldite for serial sectioning and electron microscopy.

Ultrathin (50–60 nm) sections were cut with a diamond knife on an ultramicrotome. Series of 58–220 sections were used for volumetric reconstructions. Ultrathin sections were collected on single slot grids coated with Pioloform. Serial sections were examined with a JEOL CX100 electron microscope and photographed at 5,000–16,000 times magnification at 100 kV. The 3.25×4 in. negatives were scanned at 1,200 dpi using a large-format film scanner. Images were calibrated using a diffraction grating replica photographed at the same magnification as the sections; the digitized calibration grid image was used to determine the final magnification of the digitized serial section images for each series (Fiala and Harris 2001a). Section thickness was determined by the method of cylindrical diameters (Fiala and Harris 2001b). Calibrated section images were aligned by the method of point correspondences of intrinsic fiducials (Fiala and Harris 2002). In brief, this involves identifying cross-sectioned mitochondria and other profiles on adjacent sections and computing an image transformation that aligned these points. Calibration, alignment, and three-dimensional analyses were performed using the *Reconstruct* software (Fiala 2005). Colorized electron micrograph images were produced from *Reconstruct* by filling the interior of tracings drawn on the section images. Three-dimensional renderings were produced by *3D Studio MAX* from the 3D model generated by *Reconstruct* from the tracings.

Results

Amyloid plaques in dorsolateral prefrontal cortex are common to both normal aging and Alzheimer's disease (Arnold et al. 1991; Heilbroner and Kemper 1990; Lewis et al. 1987; Rogers and Morrison 1985; Sloane et al. 1997; Struble et al. 1985). To obtain cortical brain tissue well-preserved for ultrastructural analysis and computer-based reconstruction of serial sections, we selected tissue from area 8 from two 32-year-old monkeys (Peters et al. 1994). These very old monkeys exhibited frequent plaques in cortical layers II–III, consequently we selected neuritic plaques from layers II–III for detailed study.

Dystrophic neurites are diverticula

The appearance and composition of the plaques we examined were consistent with those of the primitive type described in earlier ultrastructural studies of aged monkeys

(Martin et al. 1994; Peters 1991; Struble et al. 1985; Wisniewski et al. 1973). Primitive plaques were composed of numerous dystrophic neurites interspersed among normal-looking neuronal and glial profiles (Fig. 1). Extracellular spaces between profiles were often filled with an electron-dense material containing a meshwork of fine filaments. Most swollen neuritic profiles contained mitochondria and mitochondria-sized lamellar and dense bodies of various morphologies. Other profiles contained mostly large vesicles, 50–100 nm in diameter, with both clear and dense cores. A few profiles consisted predominantly of either tubular structures 50–100 nm in diameter or small vesicles 15–25 nm in diameter, similar to the tubulovesicular structures described after blockade of anterograde axonal transport (Tsukita and Ishikawa 1980).

When followed through serial sections, the profiles of dystrophic neurites were found to be organelle-filled swellings occurring along otherwise normal neurites (e.g.

Fig. 2). In most cases the dystrophic neurite could be traced back to a structure that had a narrow diameter ($<0.25\ \mu\text{m}$) and contained just a few microtubules, characteristic of a small unmyelinated axon in cortical neuropil. But the non-swollen regions of a few neurites had larger diameters (0.3–0.4 μm) and 10 or more microtubules, consistent with profiles of either large axons or small dendrites. The existence of a synapse distant from the swelling confirmed the axonal nature of some neurites, but most reconstructed neurites did not form a synapse within the series. Although most neurites could not be definitively identified as axons or dendrites, we found no direct evidence that any of the dystrophic neurites were dendrites.

While some dystrophic swellings were axial varicosities, three-dimensional reconstruction revealed that the organelle-filled swellings were more commonly off-shoots from the main axis of the neurite (Figs. 2b, e, 3b). The descriptive term *diverticulum* seems appropriate for these

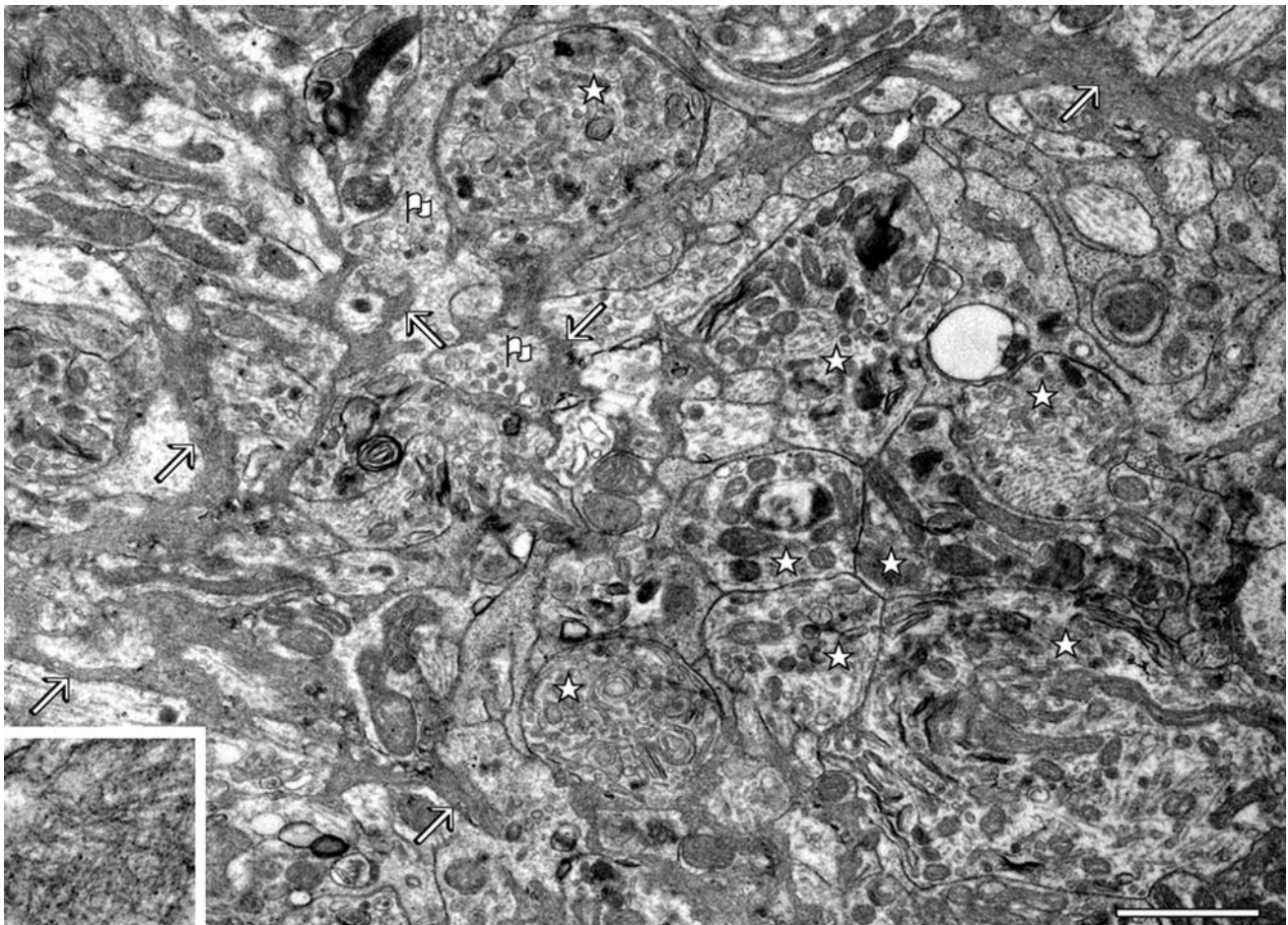


Fig. 1 Neuropil of a primitive plaque. The plaque contains large, organelle-filled profiles of dystrophic neurites (stars) interspersed among normal-looking neuronal and glial profiles. The most common inclusions in the dystrophic neurites are mitochondria, but a few dystrophic neurites exhibit a predominance of vesicular inclusions

(flags). Extending through the extracellular spaces between the profiles is an electron dense substance (arrows) that consists of a meshwork of fine filaments as shown in the inset (at twice the magnification). Scale bar 1 μm

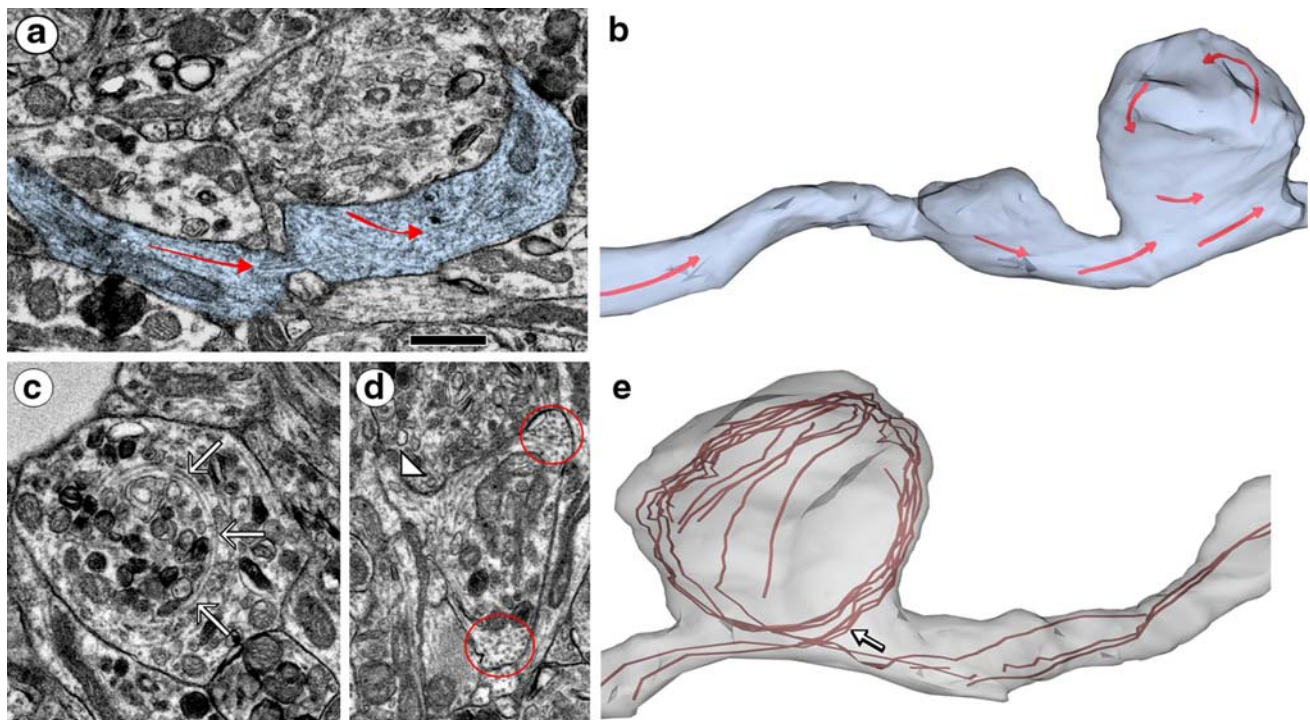


Fig. 2 Microtubules in diverticula. **a** A neurite (shaded blue) consisting of a main axis to the left and a diverticulum above the main axis on the right. The diverticulum contains numerous microtubules but few other organelles. The paths of the microtubules (red arrows) follow the main axis except in the diverticulum where they circle around in a loop. **b** Reconstruction of the neurite in **a** shows the paths of microtubules (red arrows) and their circular orientation in the diverticulum. **c** Another diverticulum in which the circular paths of the microtubules (arrows) can be seen. **d** A third diverticulum into which a few microtubules enter from the narrow

neck (arrowhead) that connects the swelling to the main axis of the neurite. The cross-sectioned microtubules at the top and bottom (red circles) form one bundle looping out of the plane of section, while the obliquely sectioned bundle near the neck loops in an orthogonal direction almost in the plane of section. **e** A different diverticulum in which some of the microtubules are partially reconstructed to show the loop circumnavigating the perimeter. Some microtubules clearly enter the loop from the main axis (arrow). Scale bar 0.5 μm for **a**, **c** and **d**

off-shoots since they appear to accumulate organelles that are normally transported along the axis of the neurite. Diverticula extending from other diverticula were also present (see below). Diverticula did not resemble growth cones since they did not exhibit filopodial extensions or an actin-rich dense cytoplasm.

Diverticula contain microtubule loops and accumulations of organelles

In normal axons and dendrites, microtubules run in a fairly straight course along the longitudinal axis and do not extend into the small protrusions formed by boutons and spines (Peters et al. 1991). In contrast, within diverticula microtubules coiled in circular loops (Fig. 2). Microtubules entering a diverticulum from the main axis crossed the paths of microtubules coiling within the diverticulum (Fig. 2b). Oblate (flattened) diverticula contained a circular bundle of microtubules (Fig. 2b, e), while more spherical diverticula often had bundles of microtubules that circled

in directions orthogonal to each other (Fig. 2d). The profiles of cross-sectioned microtubules in diverticula appeared indistinguishable from microtubule profiles in non-plaque neuropil, and had diameters of 20–25 nm consistent with normal microtubules.

Many diverticula contained large numbers of inclusions that were easily identified as mitochondria by the presence of inner and outer membranes surrounding an electron-dense matrix containing visible cristae. Sometimes microtubules and mitochondria were the only organelles present within a diverticulum (Fig. 3a, b), and the mitochondria often curved to follow the contours of the surface of the diverticulum (Fig. 3c). Three-dimensional reconstructions further revealed that some mitochondria in diverticula were complex branched structures, which contrasts with the normal cylindrical appearance of mitochondria in the main axis of the neurite (Fig. 3d).

A variety of other inclusions were also seen in diverticula, including dense bodies, vacuoles, multivesicular and tubular structures, as well as dense-core and clear vesicles. Bundles or coils of neurofilaments were not found in the

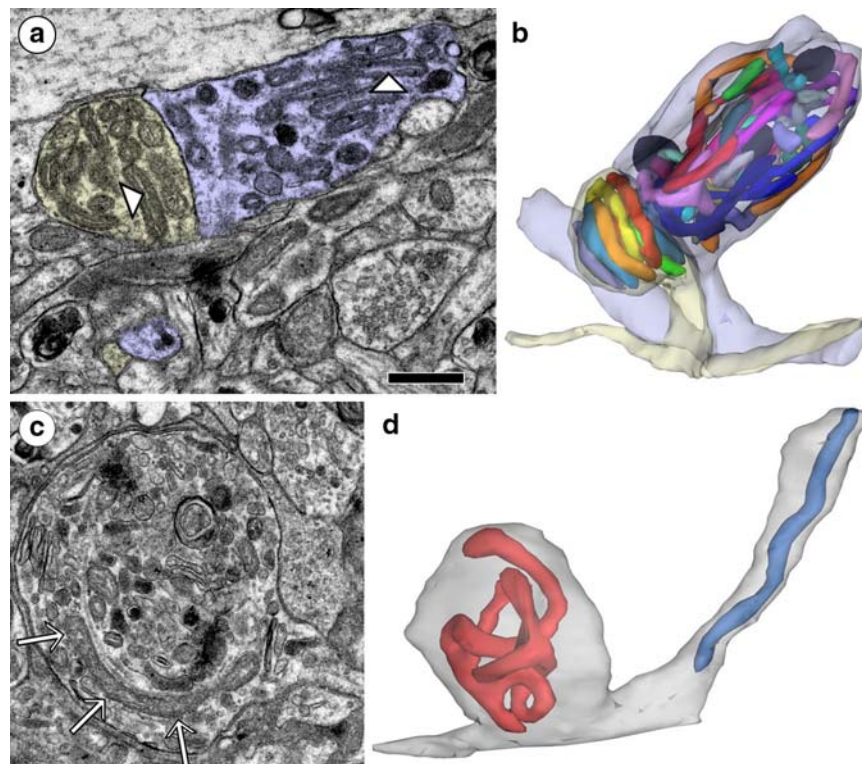


Fig. 3 Mitochondria in diverticula. **a** Two adjacent diverticula (shaded tan and purple) are filled with mitochondria. Each mitochondrion has a single longitudinally-oriented crista (arrowheads). The diverticula connect to the main axes of their neurites through thin necks, the profiles of which lie below the diverticula (shaded in lower left of **a**). **b** Three-dimensional reconstruction of the diverticula in **a** reveals the large number of inclusions that are clearly identifiable as mitochondria (different colors). In the larger diverticulum (shaded

purple) three mitochondria have a grossly distended central crista giving them a spherical shape (charcoal-colored). **c** A long, curved mitochondrion (arrows) in a different diverticulum lies adjacent to a curved microtubule. **d** Reconstruction of mitochondria in the neurite shown in Fig. 2e reveals that the mitochondrion in the main axis (blue) has a normal cylindrical shape while the mitochondrion in the diverticulum (red) is convoluted and branching. Scale bar 0.5 μm for **a**, **c**

diverticula, although bundles of intermediate filaments were readily identifiable in astrocytic processes within the plaque. Likewise, multivesicular bodies of endosomal origin (e.g. Cooney et al. 2002), while clearly identifiable in dendrites at the periphery of the plaque, were not present in substantial numbers in diverticula. Clear vesicles of the size and appearance of synaptic vesicles were not frequently seen, but when present they often occurred in swellings containing other tubulovesicular structures. No neurofibrillary tangles or paired helical filaments were encountered in the volumes that were analyzed.

Diverticula rarely formed synapses in the plaques we examined. Consequently, synapses were much less frequently found within the plaque than in the normal neuropil, consistent with earlier observations on Alzheimer's disease plaques (Kidd 1964; Krigman et al. 1965). The axons and dendrites forming synapses within the peripheral part of the plaque generally did not exhibit abnormal swellings or diverticula when reconstructed through serial sections.

Mitochondria in diverticula undergo degeneration

Mitochondria in most diverticula exhibited morphological abnormalities, suggesting that they were metabolically compromised (Frezza et al. 2006; Ghadially 1997; Karlsson and Schultz 1966). In some diverticula mitochondria appeared mostly normal, although they had a single, longitudinally-oriented crista (Fig. 3a), which is a common morphological abnormality in axonal swellings (Helen et al. 1980; Hirano 1985; Webster 1962). Occasionally the central crista was grossly swollen, creating a distorted mitochondrion that in single sections appeared as a ring-shaped profile with an electron-lucent interior (Fig. 4). Some tubular c-shaped profiles, consisting of an outer membrane surrounding an inner membrane which contained an electron-dense matrix, appeared to be grossly swollen mitochondria that had burst (Fig. 4b). In some cases, the cavity of a swollen mitochondrion contained clear vesicles and/or membranous profiles with an electron-dense inner matrix (Fig. 4c, d). Occasionally, one ring-

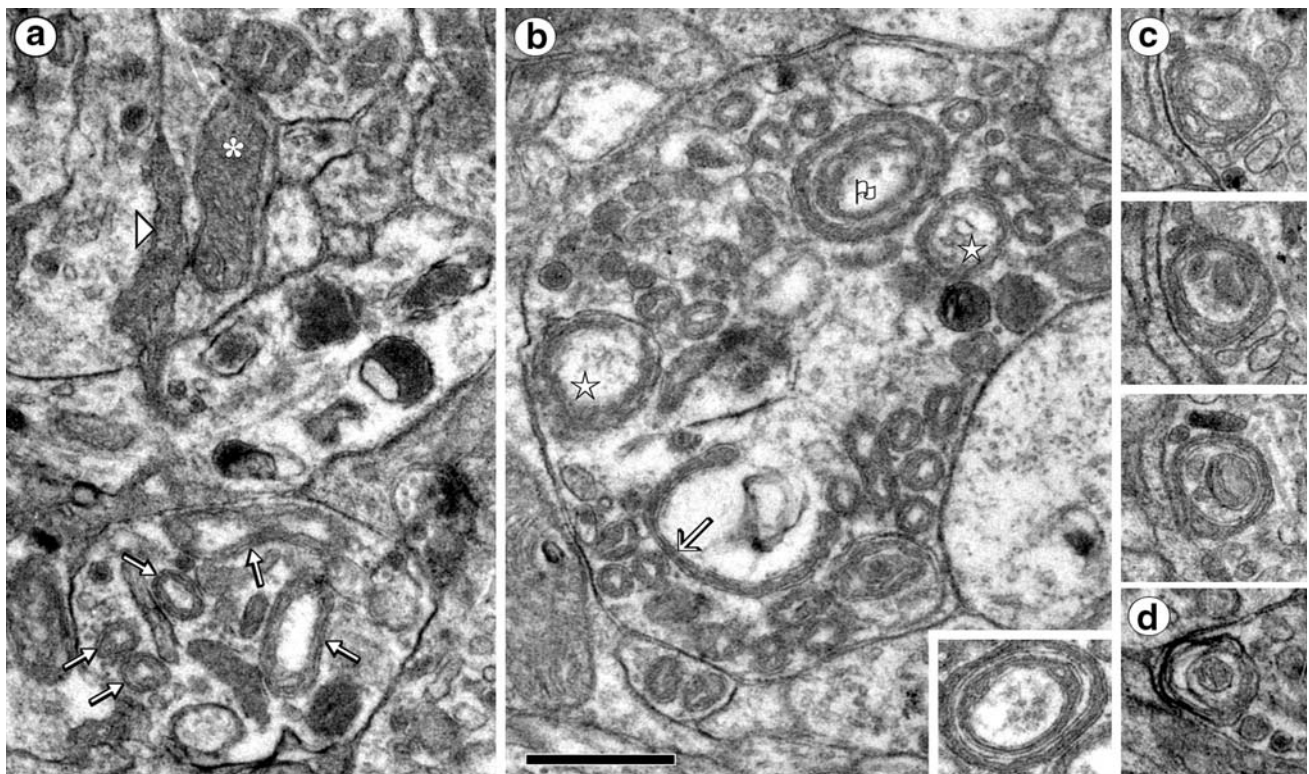


Fig. 4 Initial stages of mitochondrial degeneration. **a** A normal mitochondrion (*asterisk*) with narrow cristae in a dense matrix contrasts with the mitochondria (*arrows*) in a nearby dystrophic neurite that have dilated central cristae. The dense material in the extracellular space (*arrowhead*) is part of the wisps of extracellular material that pervade the plaque. **b** A diverticulum containing numerous mitochondria with dilated central cristae, some of which are swollen into ring-shaped profiles (*stars*). One of these consists of

two concentric ring-shaped profiles (*flag*). The *inset* image, taken from an adjacent section, shows more clearly the concentric membranes of this double ring. Another ring (*arrow*) is broken creating a narrow, c-shaped tubular profile. **c** Three sequential sections through a swollen mitochondrion with clear and dense membranous profiles located inside the ring. **d** A ring-shaped mitochondrion exhibiting further progression to a form with loose lamellae. Scale bar 0.5 μm

shaped profile occurred within another ring-shaped profile (Fig. 4b). In these double-ringed profiles, each ring had a dense inner matrix sandwiched between outer and inner pairs of membranes (Fig. 4b inset). These complex alterations in mitochondria suggest that many of the other types of profiles in diverticula, such as multivesicular and tubular vacuoles, probably arise from the degeneration of mitochondria.

To varying degrees, degenerating mitochondria were composed of membranes layered as concentric spheres (Fig. 4b–d), consistent with autophagic degradation (Hariri et al. 2000; Nixon et al. 2005). In some cases these structures consisted of an outer membrane or ring enclosing numerous lamellae and/or filaments (Fig. 5). Following these profiles through serial sections confirmed that the lamellae were completely enclosed by a bounding membrane, rather than being whorls of endoplasmic reticulum or plasma membrane. In high magnification images the internal structure of these objects often had the appearance of numerous wavy lines that came together at

two poles of the object. As many as three-dozen lines could be counted in a single profile (Fig. 5c). These lines were approximately 5 nm in width, and occasionally appeared to cross each other within a 50 nm-thick section (Fig. 5b, d), suggesting that they were either narrow ribbons or filaments.

The lamellar bodies resulting from mitochondrial degeneration sometimes clumped together creating clusters with the appearance of a bunch of grapes (Fig. 6). These clusters were typically about 1 μm in diameter and comprised of 4–40 round lamellar bodies. Most of these clusters did not appear to be surrounded by membrane, but the lamellar bodies were tightly packed together. Clusters were found in a small proportion of diverticula. In addition to a cluster, most of these diverticula also contained relatively normal-looking mitochondria. In some diverticula the clusters had a more diffuse and filamentous appearance (Fig. 6a), with no bounding membrane and 5 nm-wide filaments extending from the cluster into the cytoplasm (Fig. 6a inset).

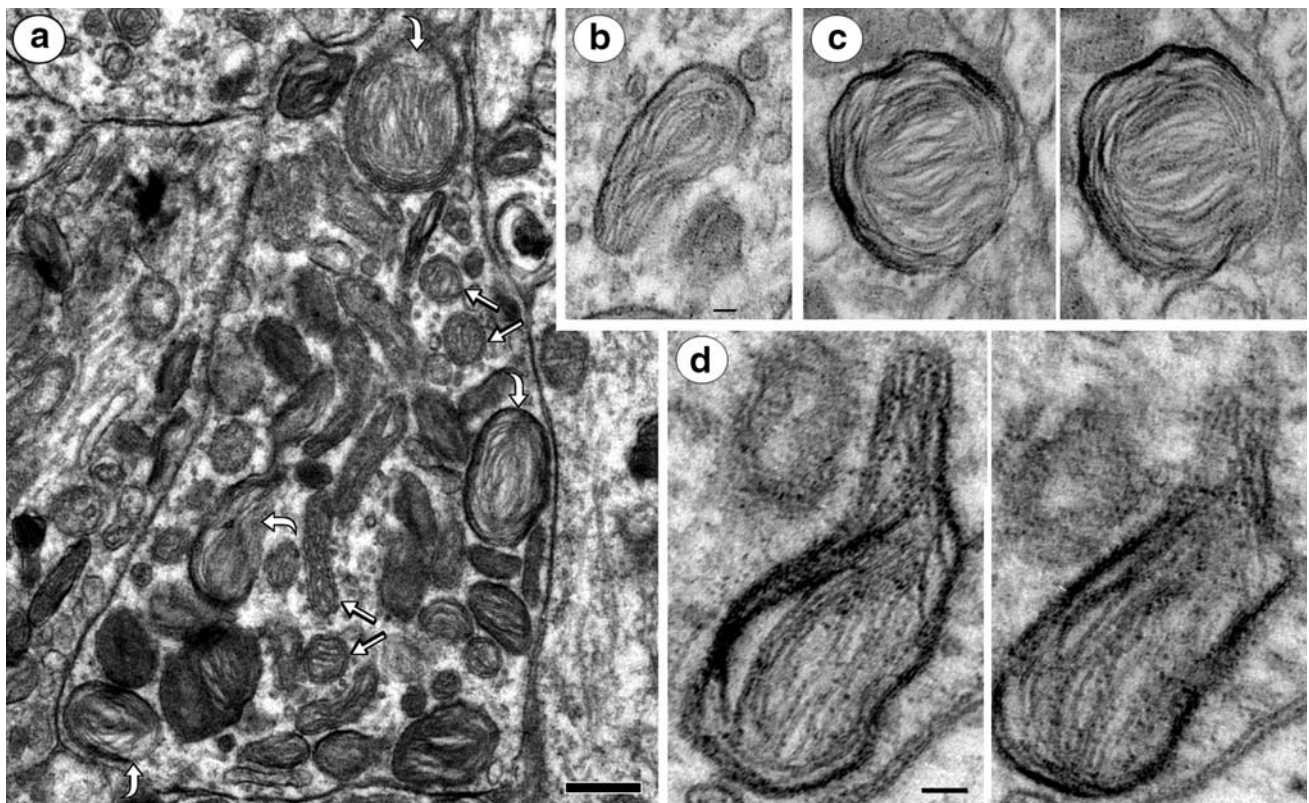


Fig. 5 Intermediate stages of mitochondrial degeneration. **a** A diverticulum containing relatively normal-looking mitochondrial profiles (*straight arrows*) and degenerating profiles (*curved arrows*) with a lamellar or filamentous interior. *Scale bar* 0.25 μm . **b** A degenerating profile photographed at higher magnification reveals interior filaments or ribbons that are no more than 5 nm wide. *Black*

scale bar 50 nm in length and 5 nm in width applies also to **c**. **c** Two adjacent sections through a spherical inclusion with parallel and crossing lines that come together at the two poles of the sphere. **d** Two adjacent sections of another inclusion at even higher magnification show that the internal lines cross each other within the 50 nm thickness of the section. *Scale bar* is 50 nm long and 5 nm wide

Lipofuscin granules were seen in cell bodies outside the plaque, as is common in aged monkeys (Peters 1991). An occasional lipofuscin-like inclusion was also found in plaque diverticula (Fig. 7). These inclusions were about the same size as the clusters of lamellar bodies but had a denser composition and included medium density vacuoles characteristic of lipofuscin granules. A lipofuscin-like inclusion in a diverticulum could have originated from one of the lamellar body clusters, given the similarities in size, shape and texture.

Extracellular material arises from intracellular sources

Diverticula had an electron-lucent cytoplasm surrounded by a heavily-stained plasma membrane that could be followed through serial sections. However, a few areas of the plaque consisted of degenerating organelles embedded entirely in an electron-dense filamentous substrate (Figs. 6a, 8). These were either severely degenerated dystrophic neurites or organelles embedded in the dense

extracellular material of the plaque. In most such cases, a bounding membrane enclosing these regions could not be discerned in single sections, nor was it possible to connect these regions to neuronal or glial processes by three-dimensional reconstruction (Fig. 8). Rather, the filamentous substrate of these regions appeared to be continuous with the filamentous material present within the extracellular spaces of the plaque. Such degenerated diverticula may represent situations in which the breakdown of the plasma membrane leads to deposition of degenerating organelles and filamentous material in the extracellular space.

Discussion

The results show that the swollen profiles of dystrophic neurites in senile plaques often extend from otherwise normal neurites. Some of these neurites were clearly axonal but the identity of others was uncertain. Studies of plaques in Alzheimer's disease or transgenic mouse models of

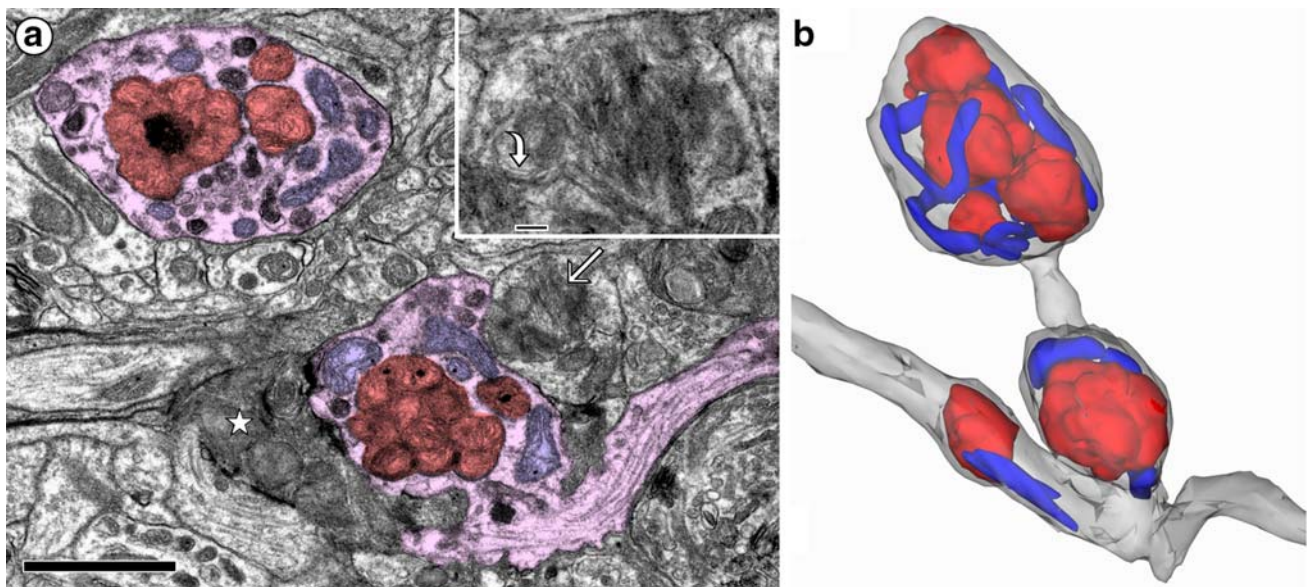


Fig. 6 Late stages of mitochondrial degeneration in diverticula. **a** A double diverticulum (*pink shading*) contains degenerated mitochondria clumped together in clusters (*red shading*) along with relatively normal-looking mitochondria (*blue shading*). Another diverticulum contains a cluster (*arrow*) with a more disorganized and diffuse meshwork of fine filaments. This is seen more clearly in the adjacent section shown in the *inset*, where 5 nm filaments (*black bar* is 5 nm × 100 nm) can be seen lying free in the cytoplasm (*curved*

arrow). A region (*star*) of densely-packed material similar in texture to the clusters does not appear to be entirely bounded by a cell membrane when viewed through serial sections. *Scale bar* 1 μm. **b** Reconstruction of the neurite shaded in **a** shows the distribution of the degenerating clusters (*red*) and the normal mitochondria (*blue*). Note that one cluster resides in the main axis of the neurite while the others are in the diverticula

Alzheimer's disease indicate that while both axons and dendrites are affected in amyloid plaques, the majority of swellings are from axons (Benes et al. 1991; Boutajangout

et al. 2004; Spires et al. 2005; Tsai et al. 2004). Our results are consistent with these light microscopic studies of amyloid pathology, and with other studies of aging which find frequent dystrophic axons throughout the cortex (Braak 1979; Kawarabayashi et al. 1993; Martin et al. 1991).

Diverticula containing only microtubules may represent the earliest pathology, since some diverticula contained coiled microtubules but few other organelles. Microtubules are the substrate for fast transport of organelles, and

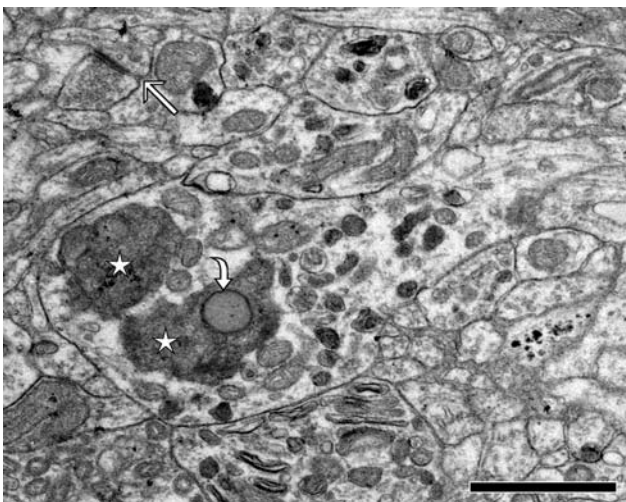
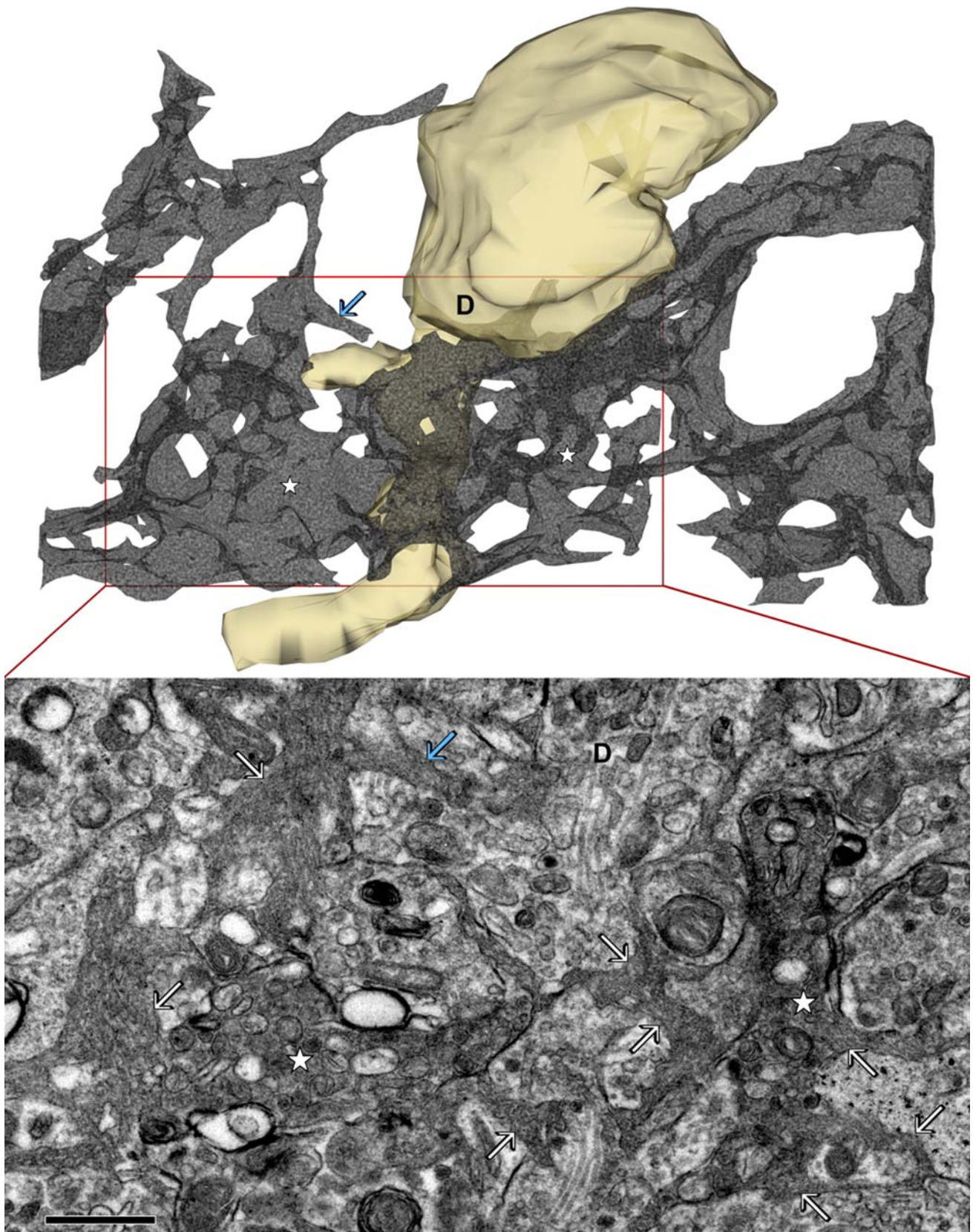


Fig. 7 A lipofuscin-like inclusion in a diverticulum. Two dark inclusions (*stars*) in a diverticulum have the appearance of lipofuscin with medium density vacuoles (*curved arrow*). This particular diverticulum also has the uncommon characteristic of containing many dense and multivesicular bodies that may be late endosomes or lysosomes. Near the diverticulum, at the periphery of the plaque, is a synapse (*arrow*) between a normal-looking bouton and dendritic spine. *Scale bar* 1 μm

Fig. 8 Degenerating diverticula. Reconstruction of a portion of a plaque shows how the dense material in the extracellular space is intermingled with what appears to be disintegrating diverticula. As shown in the micrograph taken from the rectangular area outlined on the reconstruction, regions of electron dense material are readily distinguished from a diverticulum (D) with a more lucent cytoplasm and clear plasma membrane. The same point on the electron dense material is marked with a *blue arrow* both in the reconstruction and the micrograph. In the micrograph, regions containing disordered organelles (*stars*) are embedded in a dark, filamentous matrix similar in appearance to the extracellular filamentous material (*arrows*) that extends between dystrophic neurites throughout the plaque, and no membrane can be discerned separating the extracellular material from these regions. With three-dimensional reconstruction, the shape of the dark regions with embedded organelles is seen to have a different morphology from the smooth, convex shape of a diverticulum. Holes in the dense material of the reconstruction represent the locations of other neurites and diverticula. *Scale bar* 0.5 μm



microtubule loops may cause organelles normally transported along the main axis of the neurite to be shunted into diverticula. Video microscopy of living neurons has shown that normal mitochondria are transported along the axon in an anterograde direction, but when they become metabolically impaired they switch to retrograde transport, returning to the soma for degradation (Pilling et al. 2006). Microtubule loops may hinder retrograde recycling of dysfunctional mitochondria by forming circular transport pathways that effectively trap mitochondria in diverticula. Accumulation of mitochondria and lamellar bodies in axonal swellings is consistent with the effects of blockade of retrograde axonal transport seen in other studies (e.g. Tsukita and Ishikawa 1980). Alternatively, the presence of extracellular amyloid- β in the plaque may halt the transport of mitochondria (Rui et al. 2006), leading to the formation of diverticula with accumulations of mitochondria.

Transport-impaired mitochondria may degenerate after becoming metabolically compromised, and a sufficient accumulation of degenerated mitochondria may doom the diverticulum to dissolution. Other studies have provided evidence of neuronal lysis in plaques, with neuronal cytoplasmic proteins, mRNAs, and membranous organelles found among the extracellular amyloid (Ginsberg et al. 1999; Praprotnik et al. 1996b). We likewise saw evidence of membranous organelles intermixed with the extracellular dense material, indicating that dystrophic neurites may undergo dissolution in plaques. If the intracellular material released by neuritic lysis were toxic to mitochondrial transport in nearby neurites, e.g. by containing amyloid- β (Busciglio et al. 1995; Rui et al. 2006), then progressive plaque growth could occur through continual formation and dissolution of diverticula. This would explain why dystrophic neurites occur in localized clumps in the form of neuritic plaques, but leaves unanswered the question of what initiates the pathogenesis.

One possible initial trigger for neurite swelling could be disorganization of microtubules. After ischemic injury to dendrites, for example, there is disassembly of microtubules and reassembly in unusual locations and orientations, including within dendritic spines where microtubules are not normally found (Fiala et al. 2003). If this type of repolymerization leads to loops of microtubules, a diverticulum capable of trapping organelles might be created. In support of the possibility of abnormal repolymerization of microtubules in axons, we note that coiled microtubules occur in the presynaptic compartments of prepared synaptosomes, even though microtubule loops are rarely found in the boutons of intact axons (Chan and Bunt 1978; Gordon-Weeks et al. 1982). Microtubule loops and coils have also been reported in neurite growth cones during pauses in outgrowth (Dent et al. 1999; Lankford and Klein 1990), and in developing fly neuromuscular junction (Roos

et al. 2000). Even a single microtubule loop might be sufficient to initiate the formation of a diverticulum with large numbers of coiled microtubules, because microtubule segments are transported along axons through the same fast transport mechanisms as other organelles (Baas et al. 2006).

The stages of formation of lamellar bodies indicate that mitochondria in diverticula are undergoing a type of macroautophagy, as noted in earlier ultrastructural studies (Kidd 1964; Suzuki and Terry 1967; Terry and Wisniewski 1970, 1972). Autophagy is the normal sequestration mechanism for delivery of mitochondria to lysosomes (for reviews see Brunk and Terman 2002; Kim et al. 2007). In axons, lamellar autophagic vacuoles undergo retrograde transport along axons toward the soma (Hollenbeck 1993). Delivery to the cell body is required for maturation of these autophagosomes by fusion with somal lysosomes containing acid hydrolases. Because axonal transport is disrupted in diverticula, it is likely that the autophagosomes contained therein do not receive the lysosomal enzymes required for complete digestion. Inhibition of lysosomal enzymes can lead to accumulation of incompletely digested lysosomes in the neuron and induction of tauopathy (Bi et al. 1999; Yong et al. 1999). The fine structure of incompletely digested lysosomes depends on what aspect of digestion is dysfunctional. For example, certain conditions lead to lipofuscin-type accumulations that are derived from incomplete mitochondrial digestion (Cao et al. 2006; Elleder et al. 1997; Zheng et al. 2006). Neurons in other lysosomal storage diseases accumulate lysosomes with a lamellar structure similar to the lamellar bodies in plaques (Ghadially 1997; Purpura et al. 1978). Thus, the clusters of lamellar bodies in dystrophic neurites appear to be incompletely digested autophagosomes derived from trapped mitochondria, which would be consistent with the evidence for increased mitochondrial degeneration and autophagocytosis in Alzheimer's disease (Hirai et al. 2001; Moreira et al. 2007; Nixon and Cataldo 2006). The ultimate fate of the lamellar bodies in dystrophic neurites may depend on the extent to which lysosomal enzymes are able to reach them.

Growing evidence indicates that the site of formation and aggregation of amyloid- β is intraneuronal, but exactly how this occurs is unknown. One proposed site of accumulation of amyloid- β peptides is within endosomal compartments in primary dendrites and somata of neurons, as identified by immunolabeled multivesicular bodies in single electron micrographs (Takahashi et al. 2002, 2004). This somato-dendritic amyloidogenesis is not consistent with the pathogenesis of small plaques because small plaques do not involve proximal dendrites or neuronal cell bodies (Terry and Wisniewski 1970). An immuno-electron microscopy study by another group was not able to detect

amyloid- β oligomers within endosomes in plaques (Kokubo et al. 2005c). The structural changes that we have described suggest that the filamentous material in the plaque may originate from the autophagic degeneration of mitochondria trapped in diverticula. Autophagic vacuoles are a prominent site of amyloid- β production during Alzheimer's disease or oxidative stress (Yu et al. 2005; Nixon et al. 2005; Zheng et al. 2006). Recent studies also confirm that amyloid- β precursor protein, amyloid- β peptide, and enzymes related to the production of amyloid- β from amyloid- β precursor protein, are found inside mitochondria in Alzheimer's disease and related animal models (Devi et al. 2006; Hansson et al. 2004; Kokubo et al. 2005a, b; Manczak et al. 2006). Additional support comes from immuno-electron microscopy studies showing that the amyloid- β precursor protein in dystrophic neurites is located within the lamellar dense bodies we identify as degenerating mitochondria (Boutajangout et al. 2004; Kawai et al. 1992; Martin et al. 1994).

Our observations bring together a number of apparently disparate ideas on brain amyloidosis, and indicate how disrupted axonal transport, mitochondrial malfunction and oxidative stress, macroautophagy, impaired lysosomal digestion, and intraneuronal production of amyloid- β could all contribute to amyloid plaque pathogenesis. Further study of small, nascent plaques in aging, traumatic injury, and Alzheimer's disease using three-dimensional reconstruction of fine structure may help discern additional common mechanisms of plaque initiation and evolution in these diverse conditions.

Acknowledgments This work was supported by grants from National Institute of Mental Health (RO1 MH057414) and National Institute of Neurological Disorders and Stroke (RO1 NS024760), from the National Institute on Aging (P01 AG00001), and from the Dudley Allen Sargent Research Fund, SAR, Boston University.

References

- Armstrong RA (1998) Beta-amyloid plaques: stages in life history or independent origin? *Dement Geriatr Cogn Disord* 9:227–238
- Arnold SE, Hyman BT, Flory J, Damasio AR, Van Hoesen GW (1991) The topographical and neuroanatomical distribution of neurofibrillary tangles and neuritic plaques in the cerebral cortex of patients with Alzheimer's disease. *Cereb Cortex* 1:103–116
- Baas PW, Vidya Nadar C, Myers KA (2006) Axonal transport of microtubules: the long and short of it. *Traffic* 7:490–498
- Benes FM, Farol PA, Majocha RE, Marotta CA, Bird ED (1991) Evidence for axonal loss in regions occupied by senile plaques in Alzheimer cortex. *Neuroscience* 42:651–660
- Bi X, Zhou J, Lynch G (1999) Lysosomal protease inhibitors induce meganeurites and tangle-like structures in entorhinohippocampal regions vulnerable to Alzheimer's disease. *Exp Neurol* 158:312–327
- Boutajangout A, Authlet M, Blanchard V, Touchet N, Tremp G, Pradier L, Brion J-P (2004) Characterisation of cytoskeletal abnormalities in mice transgenic for wild-type human tau and familial Alzheimer's disease mutants of APP and presenilin-1. *Neurobiol Dis* 15:47–60
- Braak H (1979) Spindle-shaped appendages of IIIab-pyramids filled with lipofuscin: a striking pathological change of the senescent human isocortex. *Acta Neuropathol (Berl)* 46:197–202
- Brunk UT, Terman A (2002) The mitochondrial-lysosomal axis theory of aging: accumulation of damaged mitochondria as a result of imperfect autophagocytosis. *Eur J Biochem* 269:1996–2002
- Busciglio J, Lorenzo A, Yeh J, Yankner BA (1995) Beta-amyloid fibrils induce tau phosphorylation and loss of microtubule binding. *Neuron* 14:879–888
- Cao Y, Espinola JA, Fossale E, Massey AC, Cuervo AM, MacDonald ME, Cotman SL (2006) Autophagy is disrupted in a knock-in mouse model of juvenile neuronal ceroid lipofuscinosis. *J Biol Chem* 281:20483–20493
- Caspersen C, Wang N, Yao J, Sosunov A, Chen X, Lustbader JW, Xu HW, Stern D, McKhann G, Yan SD (2005) Mitochondrial A β : a potential focal point for neuronal metabolic dysfunction in Alzheimer's disease. *FASEB J* 19:2040–2041
- Chan KY, Bunt AH (1978) An association between mitochondria and microtubules in synaptosomes and axon terminals of cerebral cortex. *J Neurocytol* 7:137–143
- Coleman M (2005) Axon degeneration mechanisms: commonality amid diversity. *Nat Rev Neurosci* 6:889–898
- Cooney JR, Hurlburt JL, Selig DK, Harris KM, Fiala JC (2002) Endosomal compartments serve multiple hippocampal dendritic spines from a widespread rather than a local store of recycling membrane. *J Neurosci* 22:2215–2224
- Dent EW, Callaway JL, Szebenyi G, Baas PW, Kalil K (1999) Reorganization and movement of microtubules in axonal growth cones and developing interstitial branches. *J Neurosci* 19:8894–8908
- Devi L, Prabhu BM, Galati DF, Avadhani NG, Anandatheerthavarada HK (2006) Accumulation of amyloid precursor protein in the mitochondrial import channels of human Alzheimer's disease brain is associated with mitochondrial dysfunction. *J Neurosci* 26:9057–9068
- Elleder M, Sokolova J, Hrebicek M (1997) Follow-up study of subunit c of mitochondrial ATP synthase (SCMAS) in Batten disease and in unrelated lysosomal disorders. *Acta Neuropathol (Berl)* 93:379–390
- Fiala JC (2005) Reconstruct: a free editor for serial section microscopy. *J Microsc* 218:52–61
- Fiala JC, Harris KM (2001a) Extending unbiased stereology of brain ultrastructure to three-dimensional volumes. *J Am Med Inform Assoc* 8(1):1–16
- Fiala JC, Harris KM (2001b) Cylindrical diameters method for calibrating section thickness in serial electron microscopy. *J Microsc* 202(3):468–472
- Fiala JC, Harris KM (2002) Computer-based alignment and reconstruction of serial sections. *Microsc Anal USA Edition* 52:5–7
- Fiala JC, Kirov SA, Feinberg MD, Petrak LJ, George P, Goddard CA, Harris KM (2003) Timing of neuronal and glial ultrastructure disruption during brain slice preparation and recovery in vitro. *J Comp Neurol* 465:90–103
- Frezza C, Cipolat S, de Brito OM, Micaroni M, Beznoussenko GV, Rudka T, Bartoli D, Polishuck RS, Danial NN, Scorrano L (2006) OPA1 controls apoptotic cristae remodeling independently from mitochondrial fusion. *Cell* 126:177–189
- Ghadially FN (1997) Ultrastructural pathology of the cell and matrix. Butterworth-Heinemann, Boston
- Ginsberg SD, Crino PB, Hemby SE, Weingarten JA, Lee VM, Eberwine JH, Trojanowski JQ (1999) Predominance of neuronal

- mRNAs in individual Alzheimer's disease senile plaques. *Ann Neurol* 45:174–181
- Gordon-Weeks PR, Burgoyne RD, Gray EG (1982) Presynaptic microtubules: organisation and assembly/disassembly. *Neuroscience* 7:739–749
- Götz J, Ittner LM, Kins S (2006) Do axonal defects in tau and amyloid precursor protein transgenic animals model axonopathy in Alzheimer's disease? *J Neurochem* 98:993–1006
- Gouras GK, Almeida CG, Takahashi RH (2005) Intraneuronal A β accumulation and origin of plaques in Alzheimer's disease. *Neurobiol Aging* 26:1235–1244
- Hansson CA, Frykman S, Farmery MR, Tjernberg LO, Nilsberth C, Purgslove SE, Ito A, Winblad B, Cowburn RF, Thyberg J, Ankarcróna M (2004) Nicastrin, presenilin, APH-1, and PEN-2 form active gamma-secretase complexes in mitochondria. *J Biol Chem* 279:51654–51660
- Hariri M, Millane G, Guimond MP, Guay G, Dennis JW, Nabi IR (2000) Biogenesis of multilamellar bodies via autophagy. *Mol Biol Cell* 11:255–268
- Heilbronner PL, Kemper TL (1990) The cytoarchitectonic distribution of senile plaques in three aged monkeys. *Acta Neuropathol* 81:60–65
- Helen P, Zeitlin R, Hervonen A (1980) Mitochondrial accumulations in nerve fibers of human sympathetic ganglia. *Cell Tissue Res* 207:491–498
- Hirai K, Aliev G, Nunomura A, Fujioka H, Russell RL, Atwood CS, Johnson AB, Kress Y, Vinters HV, Tabaton M, Shimohama S, Cash AD, Siedlak SL, Harris PL, Jones PK, Petersen RB, Perry G, Smith MA (2001) Mitochondrial abnormalities in Alzheimer's disease. *J Neurosci* 21:3017–3023
- Hirano A (1985) Neurons, astrocytes, and ependyma. In: Davis RL, Robertson DM (eds) *Textbook of neuropathology*, Williams and Wilkins, Baltimore, pp 1–91
- Hollenbeck PJ (1993) Products of endocytosis and autophagy are retrieved from axons by regulated retrograde organelle transport. *J Cell Biol* 121:305–315
- Karlsson U, Schultz RL (1966) Fixation of the central nervous system for electron microscopy by aldehyde perfusion. III. Structural changes after exsanguinations and delayed perfusion. *J Ultrastruct Res* 14:47–63
- Kawai M, Cras P, Richey P, Tabaton M, Lowery DE, Gonzalez-DeWhitt PA, Greenberg BD, Gambetti P, Perry G (1992) Subcellular localization of amyloid precursor protein in senile plaques of Alzheimer's disease. *Am J Pathol* 140:947–958
- Kawarabayashi T, Shoji M, Yamaguchi H, Tanaka M, Harigaya Y, Ishiguro K, Hirai S (1993) Amyloid beta protein precursor accumulates in swollen neurites throughout rat brain with aging. *Neurosci Lett* 153:73–76
- Kidd M (1964) Alzheimer's disease—an electron microscopical study. *Brain* 87:307–320
- Kim I, Rodriguez-Enriquez S, Lemasters JJ (2007) Selective degradation of mitochondria by mitophagy. *Arch Biochem Biophys* 462:245–253
- Kimura N, Tanemura K, Nakamura S, Takashima A, Ono F, Sakakibara I, Ishii Y, Kyuwa S, Yoshikawa Y (2003) Age-related changes of Alzheimer's disease-associated proteins in cynomolgus monkey brains. *Biochem Biophys Res Commun* 310:303–311
- Krigman MR, Feldman RG, Bensch K (1965) Alzheimer's presenile dementia: a histochemical and electron microscopic study. *Lab Invest* 14:381–396
- Kokubo H, Kaye R, Glabe CG, Saido TC, Iwata N, Helms JB, Yamaguchi H (2005a) Oligomeric proteins ultrastructurally localize to cell processes, especially to axon terminals with higher density, but not to lipid rafts in Tg2576 mouse brain. *Brain Res* 1045:224–228
- Kokubo H, Kaye R, Glabe CG, Yamaguchi H (2005b) Soluble Abeta oligomers ultrastructurally localize to cell processes and might be related to synaptic dysfunction in Alzheimer's disease brain. *Brain Res* 1031:222–228
- Kokubo H, Saido TC, Iwata N, Helms JB, Shinohara R, Yamaguchi H (2005c) Part of membrane-bound Abeta exists in rafts within senile plaques in Tg2576 mouse brain. *Neurobiol Aging* 26:409–418
- Lankford KL, Klein WL (1990) Ultrastructure of individual neurons isolated from avian retina: occurrence of microtubule loops in dendrites. *Brain Res Dev Brain Res* 51:217–224
- Lewis DA, Campbell MJ, Terry RD, Morrison JH (1987) Laminar and regional distributions of neurofibrillary tangles and neuritic plaques in Alzheimer's disease: a quantitative study of visual and auditory cortices. *J Neurosci* 7:1799–1808
- Lustbader JW, Cirilli M, Lin C, Xu HW, Takuma K, Wang N, Caspersen C, Chen X, Pollack S, Chaney M, Trinchese F, Liu S, Gunn-Moore F, Lue L-F, Walker DG, Kuppusamy P, Zewier ZL, Arancio O, Stern D, Yan SS, Wu H (2004) A β directly links A β to mitochondrial toxicity in Alzheimer's disease. *Science* 304:448–452
- Manczak M, Anekonda TS, Henson E, Park BS, Quinn J, Reddy PH (2006) Mitochondria are a direct site of A β accumulation in Alzheimer's disease neurons: implications for free radical generation and oxidative damage in disease progression. *Hum Mol Gen* 15:1437–1449
- Martin LJ, Sisodia SS, Koo EH, Cork LC, Dellovade TL, Weidemann A, Beyreuther K, Masters C, Price DL (1991) Amyloid precursor protein in aged nonhuman primates. *Proc Natl Acad Sci USA* 88:1461–1465
- Martin LJ, Pardo CA, Cork LC, Price DL (1994) Synaptic pathology and glial responses to neuronal injury precede the formation of senile plaques and amyloid deposits in the aging cerebral cortex. *Am J Pathol* 145:1358–1381
- Moreira PI, Siedlak SL, Wang X, Santos MS, Oliveira CR, Tabaton M, Nunomura A, Szweda LI, Aliev G, Smith MA, Zhu X, Perry G (2007) Autophagocytosis of mitochondria is prominent in Alzheimer disease. *J Neuropathol Exp Neurol* 66:525–532
- Nixon RA, Cataldo AM (2006) Lysosomal system pathways: genes to neurodegeneration in Alzheimer's disease. *J Alzheimers Dis* 9(3 suppl):277–289
- Nixon RA, Wegiel J, Kumar A, Yu WH, Peterhoff C, Cataldo A, Cuervo AM (2005) Extensive involvement of autophagy in Alzheimer disease: an immuno-electron microscopy study. *J Neuropathol Exp Neurol* 64:113–122
- Peters A (1991) Aging in monkey cerebral cortex. In: Peters A, Jones EG (eds) *Cerebral cortex. Normal and altered states of function*, vol 9. Plenum Press, New York, pp 485–510
- Peters A, Palay SL, Webster HdeF (1991) *The fine structure of the nervous system*, 3rd edn. Oxford University Press, New York
- Peters A, Leahu D, Moss MB, McNally KJ (1994) The effects of aging on area 46 of the frontal cortex of the rhesus monkey. *Cereb Cortex* 6:621–635
- Pilling AD, Horiuchi D, Lively CM, Saxton WM (2006) Kinesin-1 and dynein are the primary motors for fast transport of mitochondria in *Drosophila* motor axons. *Mol Biol Cell* 17:2057–2068
- Praprotnik D, Smith MA, Richey PL, Vinters HV, Perry G (1996a) Filament heterogeneity within the dystrophic neurites of senile plaques suggests blockage of fast axonal transport in Alzheimer's disease. *Acta Neuropathol (Berl)* 91:226–235
- Praprotnik D, Smith MA, Richey PL, Vinters HV, Perry G (1996b) Plasma membrane fragility in dystrophic neurites in senile plaques of Alzheimer's disease: an index of oxidative stress. *Acta Neuropathol (Berl)* 91:1–5

- Purpura DP, Pappas GD, Baker HJ (1978) Fine structure of meganeurites and secondary growth processes in feline GM1-gangliosidosis. *Brain Res* 143:1–12
- Rogers J, Morrison JH (1985) Quantitative morphology and regional and laminar distributions of senile plaques in Alzheimer's disease. *J Neurosci* 5:2801–2808
- Roos J, Hummel T, Ng N, Klambt C, Davis GW (2000) *Drosophila Futsch* regulates synaptic microtubule organization and is necessary for synaptic growth. *Neuron* 26:371–382
- Rui Y, Tiwari P, Xie Z, Zheng JQ (2006) Acute impairment of mitochondrial trafficking by β -amyloid peptides in hippocampal neurons. *J Neurosci* 26:10480–10487
- Sloane JA, Pietropaolo MF, Rosene DL, Moss MB, Peters A, Kemper T, Abraham CR (1997) Lack of correlation between plaque burden and cognition in the aged monkey. *Acta Neuropathol (Berl)* 94:471–478
- Spires TL, Meyer-Luehmann M, Stern EA, McLean PJ, Koch J, Nguyen PT, Bacskai BJ, Hyman BT (2005) Dendritic spine abnormalities in amyloid precursor protein transgenic mice demonstrated by gene transfer and intravital multiphoton microscopy. *J Neurosci* 25:7278–7287
- Stokin GB, Goldstein LSB (2006) Axonal transport and Alzheimer's disease. *Annu Rev Biochem* 75:607–627
- Struble RG, Price DL Jr, Cork LC, Price DL (1985) Senile plaques in cortex of aged normal monkeys. *Brain Res* 361:267–275
- Suzuki K, Terry RD (1967) Fine structural localization of acid phosphatase in senile plaques in Alzheimer's presenile dementia. *Acta Neuropathol* 8:276–284
- Takahashi RH, Milner TA, Li F, Nam EE, Edgar MA, Yamaguchi H, Beal MF, Xu H, Greengard P, Gouras GK (2002) Intraneuronal Alzheimer abeta42 accumulates in multivesicular bodies and is associated with synaptic pathology. *Am J Pathol* 161:1869–1879
- Takahashi RH, Almeida CG, Kearney PF, Yu F, Lin MT, Milner TA, Gouras GK (2004) Oligomerization of Alzheimer's beta-amyloid within processes and synapses of cultured neurons and brain. *J Neurosci* 24:3592–3599
- Terry RD, Wisniewski HM (1970) The ultrastructure of the neurofibrillary tangle and the senile plaque. In: Wolstenholme GEW, O'Connor M (eds) *Alzheimer's disease and related conditions*. J. & A. Churchill, London, pp 145–168
- Terry RD, Wisniewski HM (1972) Ultrastructure of senile dementia and of experimental analogs. In: Gaitz CM (eds) *Aging and the brain*. Plenum Press, New York, pp 89–116
- Tomlinson BE (1992) Ageing and the dementias. In: Adams JH, Duchon LW (eds) *Greenfield's neuropathology*. Oxford University Press, New York, pp 1284–1410
- Tsai J, Grutzendler J, Duff K, Gan W-B (2004) Fibrillar amyloid deposition leads to synaptic abnormalities and breakage of neuronal branches. *Nat Neurosci* 7:1181–1183
- Tsukita S, Ishikawa H (1980) The movement of membranous organelles in axons: electron microscopic identification of anterogradely and retrogradely transported organelles. *J Cell Biol* 84:513–530
- Uno H, Alsum PB, Dong S, Richardson R, Zimbric ML, Thieme CS, Houser WD (1996) Cerebral amyloid angiopathy and plaques, and visceral amyloidosis in aged macaques. *Neurobiol Aging* 17(2):275–281
- Webster HD (1962) Transient, focal accumulation of axonal mitochondria during the early stages of Wallerian degeneration. *J Cell Biol* 12:361–383
- Wegiel J, Wang KC, Tarnawski M, Lach B (2000) Microglia cells are the driving force in fibrillar plaque formation, whereas astrocytes are a leading factor in plaque degradation. *Acta Neuropathol (Berl)* 100:356–364
- Wisniewski HM, Ghetti B, Terry RD (1973) Neuritic (senile) plaques and filamentous changes in aged rhesus monkeys. *J Neuropathol Exp Neurol* 32:566–584
- Yan SD, Xiong W-C, Stern DM (2006) Mitochondrial amyloid-beta peptide: pathogenesis or late-phase development. *J Alz Dis* 9:127–137
- Yong AP, Bednarski E, Gall CM, Lynch G, Ribak CE (1999) Lysosomal dysfunction results in lamina-specific meganeurite formation but not apoptosis in frontal cortex. *Exp Neurol* 157:150–160
- Yu WH, Cuervo AM, Kumar A, Peterhoff CM, Schmidt SD, Lee JH, Mohan PS, Mercken M, Farmery MR, Tjernberg LO, Jiang Y, Duff K, Uchiyama Y, Naslund J, Mathews PM, Cataldo AM, Nixon RA (2005) Macroautophagy—a novel Beta-amyloid peptide-generating pathway activated in Alzheimer's disease. *J Cell Biol* 171:87–98
- Zheng L, Roberg K, Jerhammar F, Marcusson J, Terman A (2006) Autophagy of amyloid beta-protein in differentiated neuroblastoma cells exposed to oxidative stress. *Neurosci Lett* 394:184–189